Biogeosciences Discuss., 9, 18571–18600, 2012
www.biogeosciences-discuss.net/9/18571/2012/
doi:10.5194/bgd-9-18571-2012

Biogeosciences Discussions

External forcings, oceanographic processes and particle flux dynamics in Cap de Creus submarine canyon, NW Mediterranean Sea

A. Rumín-Caparrós[1], A. Sanchez-Vidal[1], A. Calafat[1], M. Canals[1], J. Martín[2], P. Puig[2], and R. Pedrosa-Pàmies[1]

[1]GRC Geociències Marines, Dept. d'Estratigrafia, Paleontologia i Geociències Marines, Universitat de Barcelona, 08028 Barcelona, Spain
[2]Institut de Ciències del Mar (CSIC), Passeig Marítim de la Barceloneta 37–49, 08003, Barcelona, Spain

Received: 29 November 2012 – Accepted: 30 November 2012
– Published: 18 December 2012

Correspondence to: A. Rumín-Caparrós (arumin@ub.edu)

Published by Copernicus Publications on behalf of the European Geosciences Union.

Abstract

Atmospheric forcing during 2009–2010 and 2010–2011 winter months showed differences in both intensity and persistence that led to distinct oceanographic responses. Persistent dry northern winds caused strong heat losses (14 211 W m^{-2}) in winter 2009–2010 that triggered a pronounced sea surface cooling compared to winter 2010–2011 (1597 W m^{-2} lower). As a consequence, a large volume of dense shelf water formed in winter 2009–2010, which cascaded at high speed (up to ∼1 m s^{-1}) down Cap de Creus canyon, as measured by current-meters in mooring lines deployed inside the canyon at 300 m and 1000 m water depth. The lower heat losses recorded in winter 2010–2011, together with an increased river discharge, resulted in lowered density waters over the shelf, thus preventing the formation of dense shelf water.

Particle fluxes were concurrently measured by using sediment traps at the same mooring stations. High total mass fluxes (up to 84.9 g m^{-2} d^{-1}) recorded in winter 2009–2010 indicate that dense shelf water cascading resuspended and transported sediments at least down to 1000 m deep within the canyon. Sediment fluxes were lower (28.9 g m^{-2} d^{-1}) under the quieter conditions of winter 2010–2011. The dominance of the lithogenic fraction in mass fluxes during the two winters points to a resuspension origin for most of the particles transported down canyon. The variability in organic matter and opal contents relates to seasonally controlled inputs associated to the plankton spring bloom during March and April of both years.

Our measurements of particle fluxes (including major components and grain size distribution), together with meteorological and oceanographic parameters such as wind speed, turbulent heat flux, near-bottom water temperature, current speed and suspended sediment concentration, during winters 2009–2010 and 2010–2011 along the Cap de Creus submarine canyon, show the important role of atmospheric forcings in transporting particulate matter through the submarine canyon and towards the deep sea.

BGD

9, 18571–18600, 2012

1 Introduction

Atmospheric-ocean interactions play a key role on the modification of oceanographic processes. Shifts in wind regime and air temperature among other forcing variables in the atmosphere, trigger modifications in thermohaline properties of water, and therefore, to the hydrographic configuration of the upper part of the water column. Furthermore, there are several mechanisms that can transport and mix these atmospheric-modified shallow waters with intermediate or even deep waters. For example, cooling, evaporation or freezing in the surface layer of shallow areas of the continental shelf trigger the formation of dense water that eventually spills over the shelf edge onto the continental slope (see Ivanov et al., 2004). This causes the transmission of the atmospheric signal from shallow to deep waters within a short time range.

In the Gulf of Lion there are three major mechanisms by which superficial waters are modified and transported from the surface to deep sea regions.

The first is storm-induced downwelling. This is related to the occurrence of E-SE winds that cause increased wave height and shelf sediments resuspension. The excess of water and suspended sediment piled in the inner shelf of the GoL, together with the reinforcement of the coastal current, forces shelf waters to flow towards the southwest and sink mainly through the Cap de Creus Canyon (Palanques et al., 2008). Furthermore, E-SE winds transfer humid marine air towards the coastal relief, where the air is obstructed and results in orographic rainfall and an increase in river discharge. The arrival of riverine particles due to increased river discharge, add extra suspended sediments able to be exported towards the deep sea during E-SE storms (Palanques et al., 2006, 2008; Guillén et al., 2006; Sanchez-Vidal et al., 2012).

The second mechanism is dense shelf water cascading (DSWC). This is linked to cold, dry, and persistent N-NW winds that induce sea-atmosphere heat losses and an increase in cooling and mixing of shelf waters (Millot, 1990). As a result, shelf waters become dense and sink, overflow the shelf edge, and cascade downslope preferentially through submarine canyons until reaching its equilibrium depth (Durrieu de Madron et al., 2005).

Both mechanisms (i.e. E-SE storms and DSWC) can occur separately or in parallel, and are the responsible of the remobilization and transport of sediments to the deep sea (Canals et al., 2006; Heussner et al., 2006; Palanques et al., 2006, 2008; Puig et al., 2008) and cause variability in the biogeochemical composition of settling particles (Sanchez-Vidal et al., 2009; Pasqual et al., 2010). The occurrence of these events represent an important source of food to the deep ecosystems and influence the ecology of its deep-sea populations as described, for instance, by Company et al. (2008) and Pusceddu et al. (2010). Furthermore, these events contribute to the transport and dispersion of persistent organic pollutants in the marine continental GoL shelf and open seawaters (Salvadó et al., 2012).

The third mechanism is deep-intermediate convection (MEDOC Group, 1970), that is caused again by the occurrence of cold, dry, and persistent N-NW winds that induce a heat and buoyancy loss of offshore waters in the Gulf of Lion, the Ligurian Sea and the Catalan Sea (Schroeder et al., 2010). This leads to mixing to great depths and homogenization of the water column in open sea regions. Recent studies have also documented the potential of such atmospheric driven phenomena to remobilize sediments at depths below 2000 m in the northwestern Mediterranean basin (Martín et al., 2010).

With the aim of investigating the relationship between atmospheric forcings and the oceanographic processes and near bottom particle fluxes, two mooring lines were deployed during two consecutive winters (2009–2010 and 2010–2011) in the Cap de Creus Canyon at 300 and 1000 m of water depth. After the experience gained during three decades of year-round continuous monitoring of hydrosedimentary processes in the western Gulf of Lion, it appeared that the most dynamic period in terms of water, sediment and organic matter export generally occurs in winter and early spring months, when dense shelf water forms and cascades downslope, occasional eastern storms lash out, and the most prominent yearly planktonic bloom takes place. That is why

BGD
9, 18571–18600, 2012

the experiment here described focuses in these months and combines atmospheric data (wind speed and direction, air temperature and heat fluxes) with measured physical parameters (near bottom temperature and current speed) and particle fluxes (total mass and main components) aiming to asses the atmospheric variables that govern sediment transport to the deep sea floor during these two winters.

2 Study area

The Gulf of Lion (GoL) is a river-dominated micro-tidal continental margin that extends from the Cap Croisette, in the northeastern corner of the GoL, to the Cap de Creus at its southwestern limit (Fig. 1). The main morphological characteristic of its sea floor is its crescent-shaped shelf and the numerous submarine canyons incising the slope and shelf-breake. The sea surface circulation in the GoL is linked to the Northern Current (NC), which in the study area manifests as a geostrophic jet flowing cyclonically along the slope over the 1000–2000 isobaths (Millot, 1999). The NC is associated to a permanent shelf-slope density front which separates shelf fresh coastal waters, directly influenced by the discharge of the Rhône River, from open-sea waters. Seasonal variations of the structure and intensity of the NC have been observed, with the current being narrower, deeper and more intense during winter (Millot, 1999).

Fresh water inputs into the GoL are mainly from three different hydrographic basins: the Alps in the northern part of the GoL (Rhône River), the Massif Central mountains (Hérault and Orb) and the Pyrenees mountains (Agly, Aude, Tech and Têt rivers). The Rhône River drains much of the water coming from the snowmelt of the Alps and its inputs represent more than the 90 % of the total annual freshwater inputs of the GoL (Bourrin et al., 2006). On the other hand, the Hérault and Orb rivers, and the Agly, Aude, Tech and Têt rivers, drain the Massif Central and the Pyrenees mountains respectively and, unlike the Rhône River, they are mainly controlled by a Mediterranean regime, with short and intense flash flood events (Serrat et al., 2001).

BGD
9, 18571–18600, 2012

External forcings, oceanographic processes, particle flux dynamics

A. Rumín-Caparrós et al.

The absence of significant tidal motions makes the combination of the atmospheric forcings (as the prevailing wind fields), the internal dynamics of the currents (and their interaction with the bathymetry) and the main rivers discharges to become the major source of variability of the oceanographic parameters in the GoL.

3 Material and methods

3.1 Sample collection and preparation

Two mooring lines were deployed from November 2009 to May 2010 and from December 2010 to June 2011 along the axis of the Cap de Creus submarine canyon (Fig. 1). Moorings were deployed at the canyon head and middle canyon course (as described by Lastras et al., 2007) at 300 and 1000 m depth, respectively, and were defined as CC300 and CC1000 according to its deploying depth. Each moored line was equipped with a PPS3 Technicap sequential sampling sediment trap with a 0.125 m^2 collecting surface and a 2.5 height/diameter ratio in its cylindrical part. Each trap was equipped with 12 receiving cups and was deployed at 25 m above the bottom with sampling intervals of 15 days. The collecting cups were filled with a buffered 5 % (v/v) formaldehyde solution in 0.45 µ filtered seawater. Each moored line included an Aanderaa RCM9 current meter deployed at 5 m above the bottom (CC300) and 23 m above the bottom (CC1000) equipped with a turbidimeter with a sampling interval of 30 min. Turbidity units, recorded in Formazin Turbidity Units (FTU), were transformed into suspended sediment concentrations (SSC) (mg L^{-1}) using the general calibration of Guillén et al. (2000). A technical failure of the current meter deployed at 1000 m in both years resulted in the complete absence of data at this water depth.

3.2 Analytical methods

After recovery, samples were processed according to a modified version of Heussner et al. (1990). Large swimming organisms were removed by wet sieving through a 1 mm

BGD
9, 18571–18600, 2012

nylon mesh, and organisms of less than 1 mm were handpicked under a microscope with fine tweezers. Samples were split into aliquots using a high-precision peristaltic pump robot and freeze-dried prior to chemical analysis.

Total carbon, organic carbon, and nitrogen contents were analyzed at the Scientific-Technical Services of the University of Barcelona using an elemental organic analyzer Thermo EA Flash 1112 (Thermo Scientific, Milan, Italy) working in standard conditions recommended by the supplier of the instrument. For the organic carbon analysis, samples were first decarbonated with repeated additions of 100 µL of 25 % HCl until no effervescence was observed. Between each acidification step a 60 °C drying lapse of 8 h was carried out. Organic matter (OM) content was calculated as twice the organic carbon content. The inorganic carbon content was calculated as total carbon minus organic carbon and the carbonate content was calculated assuming that all the inorganic carbon is contained within calcium carbonate ($CaCO_3$), using the molecular mass ratio of 100/12.

Biogenic silica was analyzed using a two-step 2.5 h extraction with 0.5 M Na_2CO_3 separated by filtration of the leachates. Si and Al contents of both leachates were analyzed with an Inductive Coupled Plasma Atomic Emission Spectroscopy (ICP-AES), correcting the Si content of the first leachate by the Si/Al ratio of the second one. Once corrected, Si concentrations were transformed to opal by multiplying by a factor of 2.4 (Mortlock and Froelich, 1989).

The siliciclastic fraction was obtained subtracting from the total mass the part corresponding to the major biogenic components, assuming that the amount of siliciclastics (%) was = 100 – (% OM + % $CaCO_3$ + % Opal).

Grain size analyses were performed on a Coulter LS 230 Laser Particle Size Analyzer after organic matter oxidation with 10 % H_2O_2.

3.3 Meteorological, hydrological and oceanographic data

The exchange of energy between the atmosphere and the sea surface takes place through turbulent and radiative energy fluxes. The turbulent energy flux (which includes

BGD
9, 18571–18600, 2012

the sensible and the latent heat fluxes, SHF and LHF, respectively) is linearly proportional to the wind speed and the air-sea temperature or humidity difference, and the radiative flux is a function of air temperature, humidity, and cloudiness (Deser et al., 2010). According to Josey (2003) and Schroeder et al. (2010), LHF control anomalies in the winter net heat exchanges in the GoL. Thus, LHF and also SHF in the study area have been acquired as part of the activities of NASA's Science Mission Directorate, archived and distributed by the Goddard Earth Sciences (GES) Data and Information Services Center (DISC). The source used has been the Modern Era Retrospective-analysis for Research and Applications (MERRA), which uses the GEOS-5 Data Assimilation System with the adoption of a joint analysis with the National Centers for Environmental Prediction (NCEP) and of a set of physics packages for the atmospheric general circulation model. The study of the sea-atmosphere interactions has been gridded from 42.1 to 43.4° N; and from 3.1 to 5° E (Fig. 1).

Significant wave height (Hs) has been obtained from the Leucate coastal buoy (Fig. 1), provided by the "Centre d'Études Techniques Maritimes Et Fluviales" (Ministère de l'Ecologie, de l'Energie, du Développement durable et de la Mer, CANDHIS, France).

Wind speed and direction have been acquired from the automatic meteorological station in Portbou (see location in Fig. 1), maintained by "Servei Meteorològic de Catalunya" (Generalitat de Catalunya).

Riverine discharges have been obtained from the "Laboratoire Hydraulique et Mesures from the Compagnie Nationale du Rhône". The rivers considered are the Rhône River, because it is the main contributor of freshwater inputs of the GoL, and the Hérault, Orb Agly, Aude, Tech and Têt rivers in order to consider the freshwater inputs from most of the small rivers opening to the GoL.

Data on concentration of the photosynthetic pigment Chlorophyll *a* (Chl *a*) have been obtained from the Goddard Earth Sciences (GES) Data and Information Services Center (DISC), using as a source the Moderate Resolution Imaging Spectoradiometer (MODIS) onboard the Aqua satellite. Chl *a* concentration is calculated using remotely

BGD
9, 18571–18600, 2012

sensed observations of the ocean surface with visible wavelength data. For our study, Chl *a* concentration has been gridded including the mooring location and most of the GoL area (Fig. 1).

4 Results

4.1 External forcings

Winter 2009–2010 in the Cap de Creus area (northern Catalonia) was characterized by very low temperatures. Air temperatures were approximately $-2\,^{\circ}$C lower than the average climatic values registered in the climatic atlas of Catalonia (Martín-Vide and Raso Nadal, 2008). Several wind episodes with N-NW winds reaching punctually speeds up to $44\,\mathrm{m\,s^{-1}}$ were recorded during late December 2009, mid January 2010 and mid February 2010. At the same time the individual terms composing turbulent heat losses (LHF and SHF) accumulated values of $14\,211\,\mathrm{W\,m^{-2}}$ through the entire winter, from November 2009 until the end of March 2010.

The second winter studied was on average $1\,^{\circ}$C warmer than the previous one. N-NW wind episodes with winds reaching punctually speeds up to $45\,\mathrm{m\,s^{-1}}$ during late December 2010 and early January 2011, and up to $40\,\mathrm{m\,s^{-1}}$ from mid January to the mid-end of February 2011 were recorded. However, strong wind events were concentrated in the first half of the winter so the accumulated turbulent heat loss for the whole winter (from November until the end of March), was $1597\,\mathrm{W\,m^{-2}}$ lower than the previous winter.

Two very important increases in the river discharge of the rivers draining the Pyrenees and the Massif Central are well distinguished in October 2010 and in March 2011 (Figs. 2d, 3c). During both events the Hérault River reached 40 and $850\,\mathrm{m^3\,s^{-1}}$, the Orb River reached 91 and $899\,\mathrm{m^3\,s^{-1}}$, the Agly River reached 741 and $635\,\mathrm{m^3\,s^{-1}}$, the Aude River reached 399 and $561\,\mathrm{m^3\,s^{-1}}$, the Tech River 239 and $512\,\mathrm{m^3\,s^{-1}}$, and the Têt 245 and $366\,\mathrm{m^3\,s^{-1}}$, respectively. Considering that the Rhône river basin is not affected by

BGD
9, 18571–18600, 2012

the Mediterranean climate characterized by its limited rainfall regime (Ludwig et al., 2003), its basal discharge was always very high compared with the rest of the rivers, presenting a much more regular flow rate during the whole period around 2000 $m^3 s^{-1}$ (Fig. 3c, e). The higher water discharge in the whole time series was registered at the very end of December 2010, with 5600 $m^3 s^{-1}$.

Maximum significant wave height (Hs) was recorded in March in both winters in the context of a reinforcement of easterly winds (Fig. 3a, b), in agreement with larger swell due to longer fetch distance of E winds. During winter 2009–2010 the maximum Hs recorded was of 4 m, while during the next winter the maximum Hs was 4.6 m.

Chl *a* concentration images showed increased pigment concentrations during March, reflecting the well-known seasonal phytoplankton bloom in the region (e.g. Estrada et al., 2011), but with different intensities in the two years considered. The phytoplanktonic production in the continental shelf was higher in March 2011 than in March 2010, especially in the area offshore Cap de Creus (Fig. 4).

4.2 Near bottom current regime and downward particle fluxes

Time series of near bottom water temperature, current speed, near bottom suspended sediment concentration (SSC), and downward particle flux are shown in Fig. 3d–g.

4.2.1 Winter 2009–2010

November 2009 was characterized by relatively stable oceanographic conditions at the CC300 station, with no major changes in near bottom water temperature and current speeds below 0.29 $m s^{-1}$. At the very end of December 2009 a drop in near bottom water temperature (to 11.98 °C) was recorded concomitantly with increased current speeds (0.77 $m s^{-1}$) and SSC (10.41 $mg L^{-1}$). This event lasted a couple of days. At the same time TMF reached 40.2 $g m^{-2} d^{-1}$ at CC300 while no significant increase was recorded at CC1000.

BGD
9, 18571–18600, 2012

In mid January 2010 near bottom water temperature decreased to 11.21 °C, and current speed and SSC increased up to $1.12\,\mathrm{m\,s^{-1}}$ and $34.68\,\mathrm{mg\,L^{-1}}$, respectively. The lower temperatures and high current speeds were maintained for approximately 16 days. Total Mass Flux (TMF) at CC300 reached only $20.1\,\mathrm{g\,m^{-2}\,d^{-1}}$ and at CC1000 increased slightly up to $14.7\,\mathrm{g\,m^{-2}\,d^{-1}}$ (Fig. 3g).

In February 2010 started the longer event, which lasted for one and a half months and was characterised by persistent low bottom water temperature (as low as 9.95 °C) and high velocities (up to $0.99\,\mathrm{m\,s^{-1}}$). SSC also increased considerably but did not reach the levels of the previous month, being almost 4 times lower. While no variation in TMF was recorded at the CC300 station, TMF at CC1000 registered a sharp increase up to values of $84.9\,\mathrm{g\,m^{-2}\,d^{-1}}$.

4.2.2 Winter 2010–2011

Even thought of lower magnitude, the second monitored winter monitored also displayed anomalies in near bottom water temperature, current speed and SSC at the CC300 station. In the end of December 2010 water temperature dropped more than 1.5 °C (to 11.49 °C) and current speed increased up to $0.68\,\mathrm{m\,s^{-1}}$ and SSC up to $14.57\,\mathrm{mg\,L^{-1}}$. These anomalies lasted for 17 days. TMF values at the CC300 and CC1000 stations increased up to $23.7\,\mathrm{g\,m^{-2}\,d^{-1}}$ and $16.6\,\mathrm{g\,m^{-2}\,d^{-1}}$, respectively (Fig. 3g).

January and February 2011 were characterized by relatively stable conditions excepting for a discrete (lasting less than 2 days) water temperature drop recorded concomitantly with increased current speeds (up to $0.71\,\mathrm{m\,s^{-1}}$) recorded in the end of January 2011. At the same time, SSC peaked at $11.53\,\mathrm{mg\,L^{-1}}$ and TMF at CC300 reached values up to $28.9\,\mathrm{g\,m^{-2}\,d^{-1}}$. No increased TMF was recorded at the CC1000 station.

In March 2011 slight temperature drops (to 11.07 °C), increased current speeds ($0.68\,\mathrm{m\,s^{-1}}$) and increased SSC ($7.37\,\mathrm{mg\,L^{-1}}$) were again recorded (Fig. 3g). TMF

BGD
9, 18571–18600, 2012

increased slightly at CC300 (up to 9.9 g m^{-2} d^{-1}) and after 15 days at CC1000 (up to 7.3 g m^{-2} d^{-1}) (Fig. 3g).

4.3 Main components of settling particles

The temporal variability of the main components (OM, $CaCO_3$ opal and siliciclastics) at the two stations during the winters studied is shown in Fig. 5. As repeatedly observed in this region, the siliciclastic component is the main contributor to TMF at all stations and at all depths (Heussner et al., 2006; Pasqual et al., 2010), representing almost 70 % of the total flux. Especially during winter 2010–2011, the siliciclastic relative abundance decreased with depth from CC300 to CC1000.

In general the OM relative abundance of TMF during both periods showed a clear temporal variability, displaying almost always higher concentrations at the CC300 station. During the first period maximum concentration values were recorded during the end of March 2010 at CC300 (up to 4.68 %) and during late April 2010 at CC1000 (up to 3.42 %). During the second winter maximum peaks were reached in late February 2011 at CC300 (4.38 %) and late April 2011 in CC1000 (3.61 %).

$CaCO_3$ relative abundance during the first winter peaked in late January and February 2010 in CC300 and late January 2010 in CC1000, and accounted for up to 30.49 % of the total flux. During the second winter values were significantly lower specially at the CC300 station, increasing in March–April 2011 up to 28.23 and 30.54 % of the CC300 and CC1000 flux.

Opal represented always less than 4 % of the mass flux. During the first winter opal relative abundance increased in December 2009 (up to 1.99 %) and March–April 2010 (up to 2.01 %) at both stations. During the second period, the seasonal increase of opal was more evident, increasing in very late April 2011 up to values of 1.93 % at CC300, and 3.43 % at CC1000.

BGD
9, 18571–18600, 2012

4.4 Grain size

During the two monitored periods, approximately 90 % of the particles were mainly silt-sized (between 4 and 63 µm) whereas 10 % of the particles where clay-sized (< 4 µm). A few samples included sand-sized particles (> 63 µm).

The grain size distribution display many fluctuations (Fig. 6). During the first winter, the low amount of mass obtained from the sediment cups at CC300 from mid January to mid April 2010 prevented grain size determination. However, the available data show coarsening of the sediments collected during the second half of December 2009 with respect to the samples collected at the beginning and at the end of the evaluated time series (very late November 2009 and early May 2010, respectively). Samples collected during February 2010 in CC1000 also displayed a clear coarsening with respect to the initial and final conditions (Fig. 6a).

During the second winter, slighter changes in the grain size distribution of the sediments collected by the sediment traps were recorded. Nevertheless, the samples collected at CC300 during mid-late January 2011 and during the first half of March 2011 displayed a clear coarsening with respect to the initial and final conditions (end of December 2010 and first half of June 2011, respectively) (Fig. 6b). No remarkable changes were recorded in CC1000 along the evaluated time series.

5 Discussion

5.1 Atmospheric forcing of particle fluxes in winter 2009–2010

Winter 2009–2010 was characterized by the occurrence of several wind storms that triggered important changes in the water column structure and the sediment transport downcayon. The northern windstorms occurring in December 2009 resulted in strong sea-atmosphere heat losses in the studied area (Fig. 2a–c). Accumulated SHF increased 640 W m^{-2} in less than two weeks (Fig. 2b), which represents an average of

Discussion Paper | Discussion Paper | Discussion Paper | Discussion Paper |

BGD

9, 18571–18600, 2012

External forcings, oceanographic processes, particle flux dynamics

A. Rumín-Caparrós et al.

sensible heat losses of 58 $W\,m^{-2}$ per day. These values are higher than those reported by Schroeder et al. (2010) for "normal" winters in the nearby convection zone where most extreme heat losses are believed to occur (42–43° N, 4–5° E). Consequently, at the end of December 2009 shelf waters lost temperature, became denser and sank overflowing the shelf edge and cascading downslope through the Cap de Creus submarine canyon, as shown by the decrease in near bottom water temperature at the upper canyon. This process, known as DSWC, has been recently studied in detail in several papers (e.g. Canals et al., 2006; Heussner et al., 2006; Palanques et al., 2006). The DSWC event started in December 2009, lasted for about 2 months and was formed by 3 main pulses of water.

The first DSWC pulse was recorded at the end of December 2009. This event increased down-canyon suspended sediment fluxes mainly by increasing the current speed up to 0.77 $m\,s^{-1}$ and caused an increase in the TMF up to 40.2 $g\,m^{-2}\,d^{-1}$ at CC300 (Fig. 3e, g). In addition, grain size distribution of the particles collected by the sediment trap display a clear coarsening during this pulse (Fig. 6a). This means that the cascading currents where strong enough to resuspend and transport coarse particles in suspension from the shelf downwards the basin. Nevertheless, currents were not strong enough to transport sediment deeper in the canyon, as suggested by the low TMF measured at CC1000. Overall, data suggest that the sediment eroded and transported by the dense water plume settled in some place between CC300 and CC1000.

From the end of December 2009 to mid January 2010, several cold and dry northern windstorms with high wind speeds led to a continued period of heat losses. This sustained heat loss triggered a continued cooling of the surface waters and thus a loss of buoyancy. In consequence, DSWC was reactivated in mid January as confirmed by the decrease in the near bottom water temperature and the sharp increase in the current speed and in the SSC at CC300. The strong intensification in current speed (up to 1.12 $m\,s^{-1}$) and in SSC (up to 34.68 $mg\,L^{-1}$) denoted a major escape of resuspendible fine sediments from the shelf and down the canyon. Furthermore, the TMF at both CC300 and CC1000 increased slightly evidencing that, this time, cascading waters reached probably the middle canyon course. In addition, the coarsening of the samples collected during this event at CC1000 corroborates that effectively, the cascading waters flowed downcanyon arriving to depths of at least 1000 m of water depth.

The third DSWC pulse started February 2010. At this stage, the superficial waters of the GoL were probably completely unstratified as a result of the continued wind cooling and mixing processes that took place along the winter. Winter accumulated SHF in the beginning of February was higher than 520 W m^{-2} (note the high slope of SHF in February 2010, Fig. 2b) and the accumulated turbulent heat losses were around 11 000 W m^{-2}. This might have caused surface water temperature to decrease and pronounced buoyancy losses of the coastal waters of the GoL. This situation led to shelf waters to cascade downslope continuously for a prolonged time period (from the beginning of February 2010 until the beginning of March 2010), as can be seen by the long and marked drop in near bottom water temperature (of more than 3 °C) and the notably increase of the current speed at the upper canyon (Fig. 3d, e). However, this event increased poorly down-canyon suspended sediment fluxes at CC300. Guillén et al. (2006) suggested that the “memory” of the past events on the shelf plays a crucial role in sediment dynamics as the recurrence of the preceding storms reduces the availability of fresh resuspendible shelf sediments. This suggests that those events in December 2009 and January 2010 cleaned erodible sediments in the upper canyon and thus cascading waters in February flowed without a significant suspended sediment transport to CC300 (Fig. 3g). However, cascading waters may have eroded part of the sediments trapped between the two moorings in the upper-middle canyon thus triggering an increased arrival of particles, with the maximum fluxes recorded, at the CC1000 station (Fig. 3g). This is also confirmed by grain size distribution of particles settling during that event, showing again a coarsening when compared to the pre- and post-winter conditions (Fig.6a). Overall, results demonstrate the multi-step sediment transport by cascading pulses, first from the shelf to the upper canyon, and then from the upper canyon to the middle canyon, as observed in winter 2006 by Pasqual et al. (2011) and Palanques et al. (2012). In addition, the arrival of resuspended particles

BGD
9, 18571–18600, 2012

through the southern flank of the canyon may have caused TMF to increase only at middle canyon depths and not at the canyon head (Canals et al., 2006). Even though with decreasing current speeds (and thus with decreasing capacity of eroding sediments), the DSWC pulse triggered another increase in TMF at the CC1000 station in the end of March 2010, at the very end of the cascading event.

5.2 Atmospheric forcing of particle fluxes in winter 2010–2011

An eastern windstorm with high E winds and Hs up to 3.9 m affected the Cap de Creus area in fall 2010. This episode was followed by increased river discharge in the rivers adjacent to the study area, that altogether reached 1661 $m^3 s^{-1}$ (Fig. 3c). As the mooring lines were not yet deployed we cannot investigate the impact of this eastern storm in the sediment transport downcanyon.

The following months were characterized by the occurrence of cold and dry northern windstorms. Accumulated turbulent heat fluxes from the beginning of November 2010 to late December 2010 were about 400 $W m^{-2}$ higher than during the same months the previous winter. Heat loss triggered a loss of buoyancy and the occurrence of DSWC along the submarine canyon. In fact, it seems that there is a certain heat loss threshold from which DSWC occur as can be seen comparing both winters evaluated (Fig. 2a–b). During the first winter it was not until turbulent heat fluxes (Fig. 2c) reached values about 6000 $W m^{-2}$ when the first DSWC event occurred. Similarly occurred during winter 2010–2011, when winter accumulated turbulent heat fluxes reached values around 6000 $W m^{-2}$ (Fig. 2c) the first dense shelf water pulse was recorded as a near bottom water temperature drop.

The DSWC event of December 2010 lasted for 17 days and triggered increased current speeds. The consequences of this event were a rapid but discrete increase in the current speed, SSC and TMF in the canyon head (Fig. 3e–g). Furthermore, the newly formed water plume become dense enough to cascade along the canyon arriving to depths of at least 1000 m as the TMF of the CC1000 recorded values of approximately 16.6 $g m^{-2} d^{-1}$ (Fig. 3g).

BGD
9, 18571–18600, 2012

External forcings, oceanographic processes, particle flux dynamics

A. Rumín-Caparrós et al.

Turbulent heat losses from the beginning of January until March 2011 were lower than the previous 2009–2010 winter. Furthermore, the increased river discharge recorded in the Rhône River throughout winter, together with the punctual discharge from the smaller rivers opening to the Gulf of Lion, suggest the presence of a large amounts of light freshwater in the shelf. This might have inhibited dense water formation through increasing buoyancy of surface waters.

In late January 2011 a slight temperature drop suggest the arrival of dense shelf waters. The occurrence of a concomitant eastern storm with Hs up to 3.6 m suggests that the eastern storm reactivated punctually DSWC, despite the freshwater inhibition. Indeed it is well know that eastern storm cause intense shelf sediment resuspension, that can decrease buoyancy and form a downcanyon flow (Palanques et al., 2006; Sanchez-Vidal et al., 2012). This is demonstrated by the increased current speed (0.71 $\mathrm{m\,s^{-1}}$), SSC (11.02 $\mathrm{mg\,L^{-1}}$) and TMF (up to 29.0 $\mathrm{g\,m^{-2}\,d^{-1}}$) at the canyon head. The turbid flow might have stopped before reaching the CC1000 station as no significant TMF increase was recorded. The grain size of the samples collected during this event presented a clear coarsening at CC300 but not at CC1000 (Fig. 6b).

In mid March 2011, another eastern storm occurred, with Hs of more than 4.5 m and accompanied by a significant increase in the Massif Central and Pyrenees rivers discharge (Figs. 2d, 3c). Increased current speeds (up to 0.68 $\mathrm{m\,s^{-1}}$) and SSC (up to 7.37 $\mathrm{mg\,L^{-1}}$) were recorded. The fact that flooding occurred several days after the main pulse of downcanyon sediment transport suggest again that erosion from the adjacent shelf was the main source of particles introduced in the canyon during mid March 2011 (Martín et al., this issue). The turbid flow did not penetrate into the canyon deeper than about 350 m. The coarsening of the grain size of the particles collected at CC300 suggest that near bottom currents during this event where strong enough to resuspend and transport coarse particles in suspension from the shelf to the canyon head (Fig. 6b).

5.3 Variability in composition of the settling particles and Chl *a*

5.3.1 Principal variations in the composition of the settling particles of winter 2009–2010

Winter 2009–2010 dense shelf water pulses caused TMF to increase and to be dominated by the siliciclastic fraction (more than 67 %) (Fig. 5). During December 2009, and January and February 2010, the composition of the settling particles was relatively constant, showing that DSWC pulses transported homogenized materials from the same origin (i.e. the shelf and upper slope) towards the basin (as reported before by Pasqual et al., 2010). Furthermore, during these events, the non-siliciclastic fraction was close to the values reported by Heussner et al. (2006), with ~20–30 % $CaCO_3$, 2–3 % OM, and opal was virtually absent. These values were also close to those reported by Roussiez et al. (2006) for the superficial sediments from the shelf and upper slope (31 % $CaCO_3$, 1–4 % OM and opal nearly absent or under detection limit).

In the end of the winter the changes in the composition of the settling particles responded to a seasonal control. The higher variability in the biological signal (i.e. OM and opal content) occurred in response to the biological spring bloom recorded during March and April 2010 (Fig. 4). The less severe hydrodynamic conditions (end of the major cascading pulse) also favored the reduction of the input of resuspended lithogenic particles.

The $CaCO_3$ relative abundance displayed an apparently random pattern with higher values in January and February 2010 and not related to OM and opal peaks (Fig. 5). The resuspension and transport of carbonated shells from the shelf is the most plausible explanation, as suggested by Martín et al. (2006) in the nearby La Fonera submarine canyon.

5.3.2 Composition variability of settling particles during winter 2010–2011

In the context of a milder and wetter 2010–2011 winter, the dominance of lithogenics fraction in the settling particles also suggested a dominant resuspended origin. However, primary production products (i.e. OM and opal) dilution due to increased lithogenic sediments resuspension was lower, most likely because of the weakened main transport events. This was also evident in the relative abundance of $CaCO_3$ and specially at the CC1000 station, impacted by less events than the preceding winter. The higher phytoplanktonic production probably related to a higher nutrient fertilization due to the large arrival of riverine nutrient inputs may have triggered an increase of the relative abundance of the biogenic components in the settling particles (Fig. 5).

6 Conclusions

This study compares hydro-sedimentary processes and associated particle fluxes in the westernmost submarine canyon of the Gulf of Lion, at the outlet of the shelf and slope cyclonic circulation system of the area, during the winters of 2009–2010 and 2010–2011, when contrasting atmospheric forcings developed and led to unequal modifications of the thermohaline properties of the upper ocean layer.

A more pronounced ocean to atmosphere heat transfer (up to $14\,211\,\mathrm{W\,m^{-2}}$) occurred in winter 2009–2010, which triggered a stronger cooling of the water over the continental shelf compared to winter 2010–2011. This situation resulted in an increase in the density of surface water, which sank and cascaded at higher velocities (up to $0.99\,\mathrm{m\,s^{-1}}$) down the Cap de Creus canyon. The higher current speeds recorded during winter 2009–2010 caused a higher erosion, resuspension and ultimately transport of sediment to the mid canyon reach. In contrast, during winter 2010–2011 reduced heat losses were recorded ($12\,614\,\mathrm{W\,m^{-2}}$), which together with a high volume of accumulated freshwater over the shelf, inhibited the penetration of dense shelf water down to the middle canyon. A noticeable eastern storm that occurred this winter, with

BGD
9, 18571–18600, 2012

associated peak near bottom currents of 0.68 $m\,s^{-1}$ at 300, resulted in the export of particles only down to the upper canyon reach.

The lithogenic fraction was dominant in the particle fluxes of the two winters, which point to a resuspension origin, despite the comparatively milder character of the 2010–2011 winter. The variability in OM and opal contents followed a seasonal pattern in response to the plankton spring bloom during March and April 2010 and 2011.

The $CaCO_3$ relative abundance also showed a noticeable variability both within each winter and amongst the two winters. Variability sources are, however, different. The apparently random pattern of $CaCO_3$ in 2009–2010 is attributed to the resuspension of relict carbonate shells during the multi-pulse, deep penetrating DSWC of that winter. On the other hand, the higher increase in the carbonates relative abundance in winter 2010–2011 can be explained by the higher phytoplanktonic production related to the higher nutrient fertilization that occurred during winter 2010–2011.

These results confirm that DSWC plays a key role in governing the timing, composition and volumes of particle fluxes that are exported down Cap de Creus canyon, while eastern storms similar to the one recorded in winter 2010–2011 can also contribute to enhance erosion, resuspension and the off shelf transport of particles independently of the occurrence of DSWC.

Acknowledgements. This research has been supported by the EC funded HERMIONE (FP7-ENV-2008-1-226354) and PERSEUS RTD projects (FP7 287600), and by the Spanish project GRACCIE (CSD2007-00067) and DOS MARES (CTM2010-21810-C03-01). Generalitat de Catalunya is acknowledged for support to GRC Marine Geosciences through its Grups de Recerca Consolidats grant 2009 SGR 1305. We thank D. Amblas and the crew of the vessel *Lluerna* and *Felipe* for their dedication during mooring operations. We also thank M. Guart for helping with the laboratory work, and X. Rayo for his technical assistance when using Geographic Information Systems.

References

Bourrin, F. and Durrieu de Madron, X.: Contribution of the study of coastal rivers and associated prodeltas to sediment supply in north-western Mediterranean Sea (Gulf of Lions), Vie Milieu, 56, 307–314, 2006.

Canals, M., Casamor, J. L., Urgeles, R., Farrán, M., Calafat, A. M., Amblas, D., Willmott, V., Estrada, F., Sánchez, A., Arnau, P., Frigola, J., and Colás, S.: Mapa del relleu submarí de Catalunya, 1:250 000; Institut Cartogràfic de Catalunya, Barcelona, Spain, 2004.

Canals, M., Puig, P., Durrieu de Madron, X., Heussner, S., Palanques, A., and Fabres, J.: Flushing submarine canyons, Nature, 444, 354–357, doi:10.1038/nature05271, 2006.

Company, J. B., Puig, P., Sardà, F., Palanques, A., Latasa, M., and Scharek, R.: Climate influence on deep sea populations, PloS one, 3, e1431, doi:10.1371/journal.pone.0001431, 2008.

Deser, C., Alexander, M. A., Xie, S.-P., and Phillips, A. S.: Sea Surface Temperature Variability: Patterns and Mechanisms, Ann. Rev. Mar. Sci., 2, 115–143, doi:10.1146/annurev-marine-120408-151453, 2010.

Durrieu de Madron, X., Zervakis, V., Theocharis, A., and Georgopoulos, D.: Comments to "Cascades of dense water around the world ocean", Progr. Oceanogr., 64, 83–90, doi:10.1016/j.pocean.2004.08.004, 2005.

Estrada, M.: Primary production in the Northwestern Mediterranean, Sci. Mar., 60, 55–64, 1996.

Guillén, J., Palanques, A., Puig, P., Durrieu de Madron, X., and Nyffeler, F.: Field calibration of optical sensors for measuring suspended sediment concentration in the Western Mediterranean, Sci. Mar., 64, 427–435, 2000.

Guillén, J., Bourrin, F., Palanques, A., Durrieu de Madron, X., Puig, P., and Buscail, R.: Sediment dynamics during wet and dry storm events on the Têt inner shelf (SW Gulf of Lions), Mar. Geol., 234, 129–142, doi:10.1016/j.margeo.2006.09.018, 2006.

Heussner, S., Ratti, C., and Carbonne, J.: The PPS 3 time-series sediment trap and the trap sample processing techniques used during the ECOMARGE experiment, Cont. Shelf Res., 10, 943–958, doi:10.1016/0278-4343(90)90069-X, 1990.

Heussner, S., Durrieu de Madron, X., Calafat, A., Canals, M., Carbonne, J., Delsaut, N., and Saragoni, G.: Spatial and temporal variability of downward particle fluxes on a continental

BGD
9, 18571–18600, 2012

External forcings, oceanographic processes, particle flux dynamics

A. Rumín-Caparrós et al.

slope: Lessons from an 8-yr experiment in the Gulf of Lions (NW Mediterranean), Mar. Geol., 234, 63–92, doi:10.1016/j.margeo.2006.09.003, 2006.
Ivanov, V. V., Shapiro, G. I., Huthnance, J. M., Aleynik, D. L., and Golovin, P. N.: Cascades of dense water around the World Ocean, Progr. Oceanogr., 60, 47–98, doi:10.1016/j.pocean.2003.12.002, 2004.
Josey, S. A.: Changes in the heat and freshwater forcing of the eastern Mediterranean and their influence on Deep Water Formation, J. Geophys. Res., 108, 3237, doi:10.1029/2003JC001778, 2003.
Lastras, G., Canals, M., Urgeles, R., Amblas, D., Ivanov, M., Droz, L., Dennielou, B., Fabrés, J., Schoolmeester, T., Akhmetzhanov, A., Orange, A., and García-García, A.: A walk down the Cap de Creus canyon, Northwestern Mediterranean Sea: Recent processes inferred from morphology and sediment bedforms, Mar. Geol., 246, 176–192. doi:10.1016/j.margeo.2007.09.002, 2007.
Ludwig, W., Meybeck, M., and Abousamra, F.: Riverine transport of water, sediments, and pollutants to the Mediterranean Sea, UNEP MAP Technical report Series 141, UNEP/MAP Athens, 111 pp., 2003.
Martín-Vide, J. and Raso Nadal, J. M.: Atlas climàtic de Catalunya, Període 1961–1990, Institut Cartogràfic de Catalunya, Barcelona, 2008.
Martín, J., Palanques, A., and Puig, P.: Composition and variability of downward particulate matter fluxes in the Palamós submarine canyon (NW Mediterranean), J. Mar. Sys., 60, 75–97, 2006.
Martín, J., Miquel, J. C., and Khripounoff, A.: Impact of open sea deep convection on sediment remobilization in the western Mediterranean, Geophys. Res. Lett., 37, L13604, doi:10.1029/2010GL043704, 2010.
Martín, J., Durrieu de Madron, X., Puig, P., Bourrin, F., Palanques, A., Houpert, L., Higueras, M., Sanchez-Vidal, A., Calafat, A. M., Canals, M., and Heussner, S.: Sediment transport through Cap de Creus Canyon during the CASCADE cruise in March 2011, Submitted, this issue.
MEDOC Group: Observation of formation of deep water in the Mediterranean Sea, 1969, Nature, 227, 1037–1040, 1970.
Millot, C. A.: The Gulf of Lions' hydrodynamic, Cont. Shelf Res., 10, 885–894, 1990.
Millot, C. A.: Circulation in the Western Mediterranean Sea, J. Mar. Sys., 20, 423–442, 1999.
Mortlock, R. A. and Froelich, P. N.: A simple method for the rapid determination of biogenic opal in pelagic marine sediments, Deep-Sea Res., 36, 1415–1426, 1989.

BGD
9, 18571–18600, 2012

External forcings, oceanographic processes, particle flux dynamics

A. Rumín-Caparrós et al.

Palanques, A., Durrieu de Madron, X., Puig, P., Fabres, J., Guillén, J., Calafat, A., Canals, M., Heussner, S., and Bonnin, J.: Suspended sediment fluxes and transport processes in the Gulf of Lions submarine canyons, The role of storms and dense water cascading, Mar. Geol., 234, 43–61. doi:10.1016/j.margeo.2006.09.002, 2006.

Palanques, A., Guillén, J., Puig, P., and Durrieu de Madron, X.: Storm-driven shelf-to-canyon suspended sediment transport at the southwestern Gulf of Lions, Cont. Shelf Res., 28, 1947–1956, doi:10.1016/j.csr.2008.03.020, 2008.

Palanques, A., Puig, P., Durrieu de Madron, X., Sanchez-Vidal, A., Pasqual, C., Martín, J., Calafat, A., Heussner, S., and Canals, M.: Sediment transport to the deep canyons and open-slope of the western Gulf of Lions during the 2006 intense cascading and open-sea convection period, Progr. Oceanogr., 106, 1–15, 2012.

Pasqual, C., Lee, C., Goñi, M., Tesi, T., Sanchez-Vidal, A., Calafat, A., Canals, M., and Heussner, S.: Use of organic biomarkers to trace the transport of marine and terrigenous organic matter through the southwestern canyons of the Gulf of Lion, Mar. Chem., 126, 1–12, doi:10.1016/j.marchem.2011.03.001, 2011.

Pasqual, C., Sanchez-Vidal, A., Zúñiga, D., Calafat, A., Canals, M., Durrieu de Madron, X., Puig, P., Heussner, S., Palanques, A., and Delsaut, N.: Flux and composition of settling particles across the continental margin of the Gulf of Lion: the role of dense shelf water cascading, Biogeosciences, 7, 217–231, doi:10.5194/bg-7-217-2010, 2010.

Puig, P., Palanques, A., Orange, D. L., Lastras, G., and Canals, M.: Dense shelf water cascading and furrows formation in the Cap de Creus Canyon, northwestern Mediterranean Sea, Cont. Shelf Res., 28, 2017–2030, 2008.

Pusceddu, A., Bianchelli, S., Canals, M., Sanchez-Vidal, A., Durrieu De Madron, X., Heussner, S., Lykousis, V., de Stigter, H., Trincardi, F., and Danovaro, R.: Organic matter in sediments of canyons and open slopes of the Portuguese, Catalan, Southern Adriatic and Cretan Sea margins, Deep-Sea Res., 57, 441–457, doi:10.1016/j.dsr.2009.11.008, 2010.

Ribó, M., Puig, P., Palanques, A., and Lo Iacono, C. : Dense shelf water cascades in the Cap de Creus and Palamós submarine canyons during winters 2007 and 2008, Mar. Geol., 284, 175–188, doi:10.1016/j.margeo.2011.04.001, 2011.

Roussiez, V., Ludwig, W., Monaco, A., Probst, J. L., Bouloubassi, I., Buscail, R., and Saragoni, G.: Sources and sinks of sediment-bound contaminants in the Gulf of Lions (NW Mediterranean Sea): A multi-tracer approach, Cont. Shelf Res., 26, 1843–1857, doi:10.1016/j.csr.2006.04.010, 2006.

Salvadó, J. A., Grimalt, J. O., López, J. F., Durrieu de Madron, X., Heussner, S., and Canals, M.: Transformation of PBDE mixtures during sediment transport and resuspension in marine environments (Gulf of Lion, NW Mediterranean Sea), Environ. Pollut., 168, 87–95, doi:10.1016/j.envpol.2012.04.019, 2012.
Sanchez-Vidal, A., Pasqual, C., Kerhervé, P., Heussner, S., Calafat, A., Palanques, A., Durrieu de Madron, X., Canals, M., and Puig, P.: Across margin export of organic matter by cascading events traced by stable isotopes northwestern Mediterranean Sea, Limnol. Oceanogr., 54, 1488–1500, 2009.
Sanchez-Vidal, A., Canals, M., Calafat, A., Lastras, G., Pedrosa-Pàmies, R., Menéndez, M., Medina, R., Company, J. B., Hereu, B., Romero. J., and Alcoverro, T.: Impacts on the Deep-Sea Ecosystem by a Severe Coastal Storm, PLoS one, 7, e30395, doi:10.1371/journal.pone.0030395, 2012.
Schroeder, K., Josey, S. A., Herrmann, M., Grignon, L., Gasparini, G. P., and Bryden, H. L.: Abrupt warming and salting of the Western Mediterranean Deep Water: Atmospheric forcings and lateral advection, J. Geophys. Res., 115, C08029, doi:10.1029/2009JC005749, 2010.
Serrat, P., Ludwig, W., Navarro, B., and Blazi, J. L.: Variabilité spatio-temporelle des flux de matières en suspension d'un fleuve côtier méditerranéen: la Têt (France), Spatial and temporal variability of sediment fluxes from a coastal Mediterranean river: the Têt (France), Cr. Acad. Sci. IIA, 333, 389–397, doi:10.1016/S1251-8050(01)01652-4, 2001.

BGD
9, 18571–18600, 2012

External forcings, oceanographic processes, particle flux dynamics

A. Rumín-Caparrós et al.

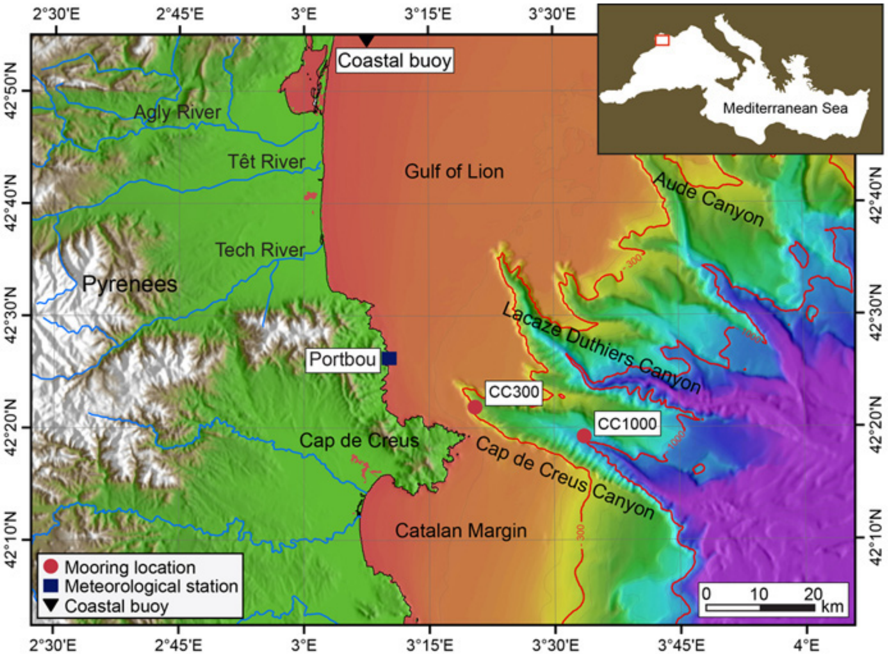

Fig. 1. Topo-bathymetric map of the Cap de Creus Canyon and neighbouring areas, at the limit between the northern Catalan margin and the Gulf of Lion (northwestern Mediterranean). Locations of moorings (dots), the meteorological station in Portbou (square) and the Leucate coastal buoy (triangle) are shown. Top-right red square indicates where the heat fluxes and Chl *a* concentration maps have been obtained. Bathymetric data published by Canals et al. (2004).

BGD
9, 18571–18600, 2012

External forcings, oceanographic processes, particle flux dynamics

A. Rumín-Caparrós et al.

Title Page
Abstract | Introduction
Conclusions | References
Tables | Figures
◀| |▶
◀ ▶
Back | Close
Full Screen / Esc
Printer-friendly Version
Interactive Discussion

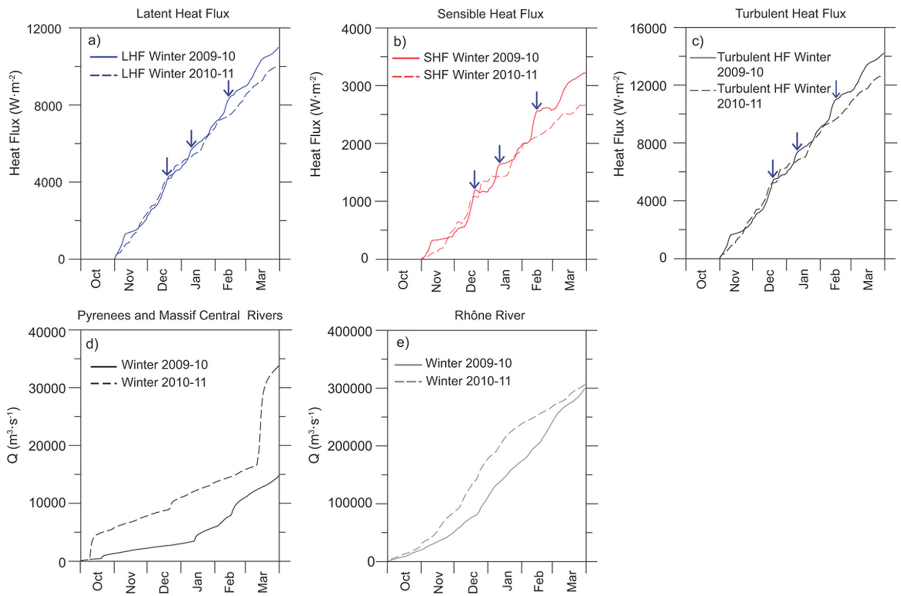

Fig. 2. (a) Accumulated Latent Heat Flux for winters 2009–2010 (continuous line) and 2010–2011 (dashed line); **(b)** accumulated Sensible Heat Flux for winters 2009–2010 (continuous line) and 2010–2011 (dashed line); **(c)** accumulated Turbulent Heat Flux for winters 2009–2010 (continuous line) and 2010–2011 (dashed line); **(d)** accumulated river discharge from the Hérault, Orb, Agly, Aude, Tech and Têt rivers for winters 2009–2010 (continuous line) and 2010–2011 (dashed line); **(e)** accumulated river discharge from the Rhône river for winters 2009–2010 (continuous line) and 2010–2011 (dashed line). Blue arrows show period of intense heat losses.

BGD
9, 18571–18600, 2012

External forcings, oceanographic processes, particle flux dynamics

A. Rumín-Caparrós et al.

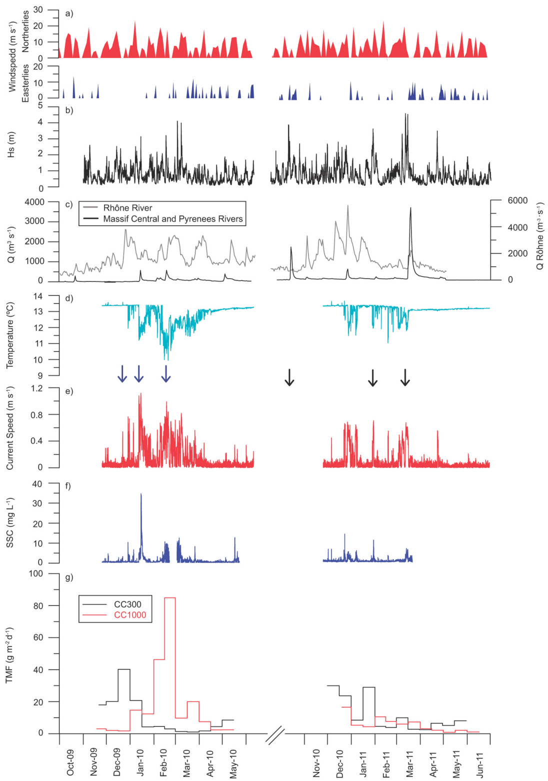

Fig. 3. **(a)** Temporal variability of northerly winds (red) and easterly winds (blue); **(b)** significant wave height (Hs); **(c)** daily fluvial discharges of the Rhône River in grey and the sum of the main small rivers flowing to the Gulf of Lions (Hérault, Orb, Agly, Aude, Tech and Têt) in black; **(d)** near-bottom temperature; **(e)** near-bottom current speed, **(f)** suspended sediment concentration (SSC) as recorded by the currentmeter at 300 m of water depth; **(g)** total mass flux at 300 (black) and 1000 m (red) of water depth. Blue arrows show period of intense heat losses (as in Fig. 2) and black arrows the occurrence of eastern storms.

BGD

9, 18571–18600, 2012

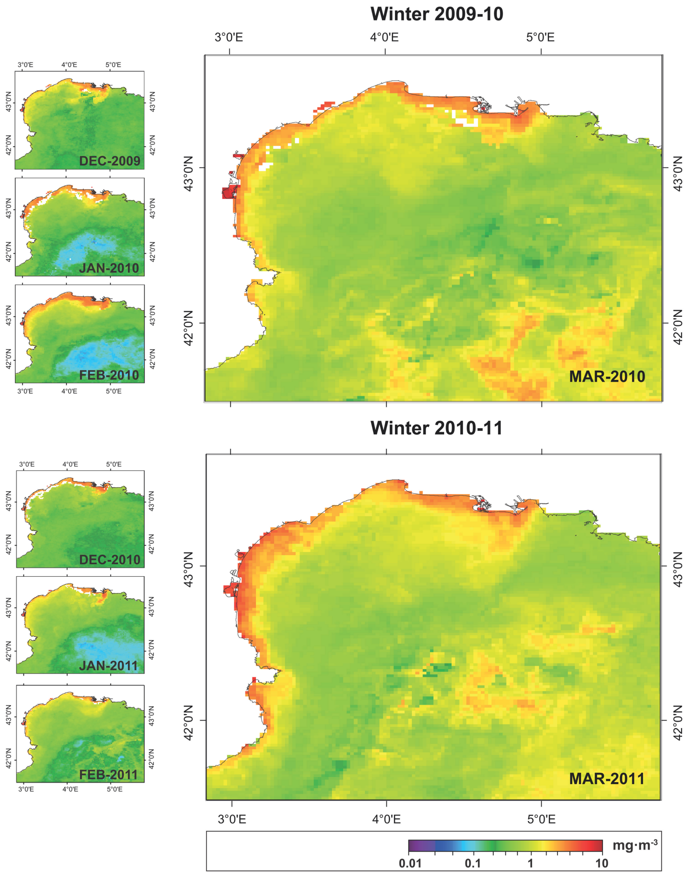

Fig. 4. Sequence of monthly mean Chlorophyll *a* concentration in the study area during both winters.

BGD
9, 18571–18600, 2012

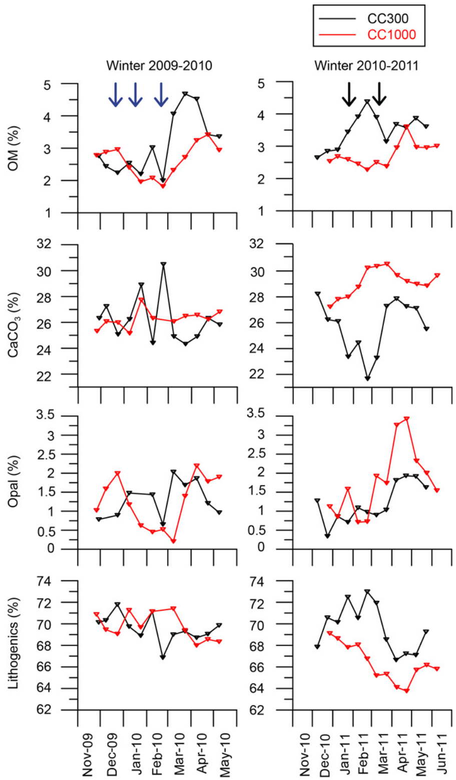

Fig. 5. Temporal variability of the main components of the settling particles ($CaCO_3$, Organic Mater (OM), opal and siliciclastics) of the two stations during the two winters studied. Black line represents the CC300 station whereas the red line represents the CC1000; **(a)** winter 2009–2010; **(b)** winter 2010–2011. Blue and black arrows show DSWC and eastern storms event (as in Figs. 2 and 3).

BGD
9, 18571–18600, 2012

External forcings, oceanographic processes, particle flux dynamics

A. Rumín-Caparrós et al.

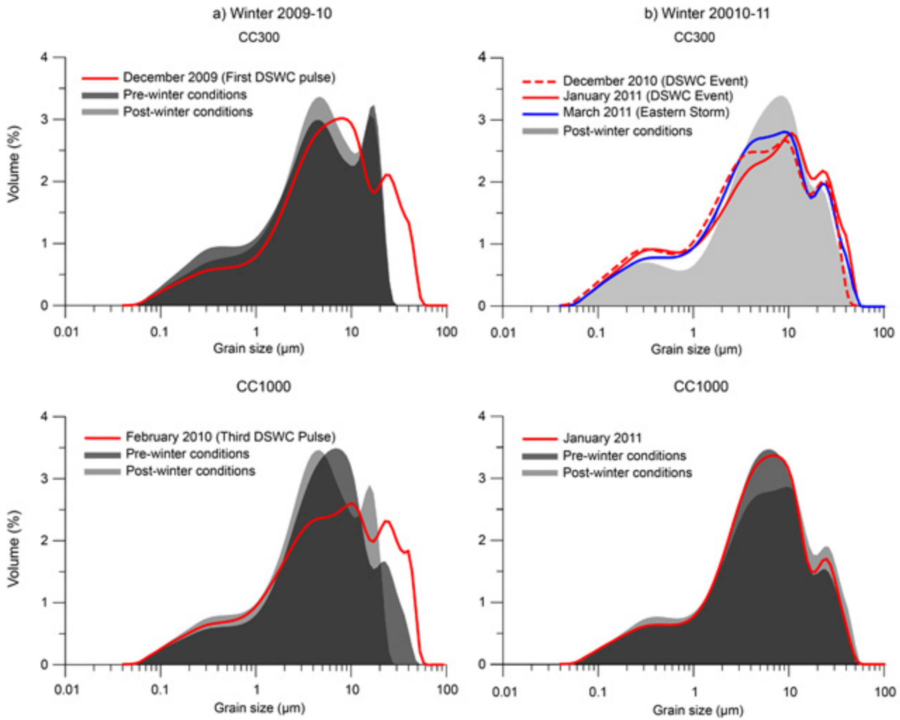

Fig. 6. Grain size distribution of sediment trap samples. In black is represented the grain size distribution at the beginning of the winter (initial conditions) and in gray the grain size distribution at the end of the winter (final conditions). Red and blue lines represent the grain size distribution during main transport events. **(a)** Grain size distribution at CC300 and CC1000 during winter 2009–2010. **(b)** Grain size distribution at CC300 (Dashed line for December 2010 DSWC event and continuous line for January 2011 DSWC event) and CC1000 during winter 2010–2011.

BGD
9, 18571–18600, 2012